

Perceptual Learned Video Compression with Recurrent Conditional GAN

Ren Yang¹, Radu Timofte^{1,2}, Luc Van Gool^{1,3}

¹ETH Zürich, Switzerland

²Julius Maximilian University of Würzburg, Germany ³KU Leuven, Belgium

ren.yang@vision.ee.ethz.ch, radu.timofte@uni-wuerzburg.de, vangool@vision.ee.ethz.ch

Abstract

This paper proposes a Perceptual Learned Video Compression (PLVC) approach with recurrent conditional GAN. We employ the recurrent auto-encoder-based compression network as the generator, and most importantly, we propose a recurrent conditional discriminator, which judges on raw vs. compressed video conditioned on both spatial and temporal features, including the latent representation, temporal motion and hidden states in recurrent cells. This way, the adversarial training pushes the generated video to be not only spatially photo-realistic but also temporally consistent with the groundtruth and coherent among video frames. The experimental results show that the learned PLVC model compresses video with good perceptual quality at low bit-rate, and that it outperforms the official HEVC test model (HM 16.20) and the existing learned video compression approaches for several perceptual quality metrics and user studies. The codes will be released at the project page: <https://github.com/RenYang-home/PLVC>.

1 Introduction

Recent years have witnessed the increasing popularity of end-to-end learning-based image and video compression. Most existing models are optimized towards distortion, *i.e.*, PSNR and MS-SSIM. Recently, Generative Adversarial Networks (GANs) have been used in image compression, to boost perceptual quality [Agustsson *et al.*, 2019; Mentzer *et al.*, 2020]. However, efficient perceptual *video* compression still remains limited.

In this paper, we propose a Perceptual Learned Video Compression (PLVC) approach with recurrent conditional GAN, in which a recurrent generator and a recurrent conditional discriminator are trained in an adversarial way for perceptual compression. The recurrent generator contains recurrent auto-encoders to compress video and generate visually pleasing reconstructions in the adversarial training. More importantly, we propose a recurrent conditional discriminator, which judges between raw and compression video conditioned on the spatial-temporal features, including latent representations, motion and the hidden states transferred through

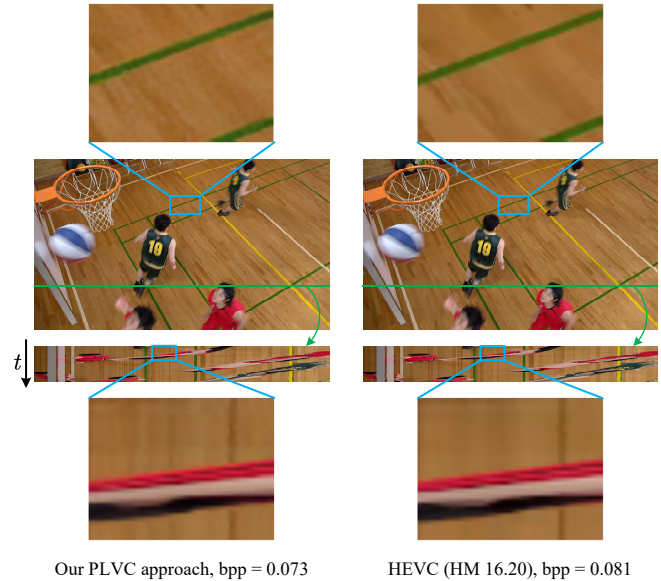


Figure 1: Example of the proposed PLVC approach in comparison with the official HEVC test model (HM 16.20).

recurrent cells. Therefore, in the adversarial training, the discriminator is able to force the recurrent generator to reconstruct both photo-realistic and temporally coherent video, thus achieving good perceptual quality.

Fig. 1 shows the visual result of the proposed PLVC approach on *BasketballDrill* (bpp = 0.0730) in comparison with the official HEVC test model HM 16.20 (bpp = 0.0813). The top of Fig. 1 shows that our PLVC approach achieves richer and more photo-realistic textures than HEVC. At the bottom of Fig. 1, we show the temporal profiles by vertically stacking a specific row (marked as green) along time steps. It can be seen that the result of our PLVC approach exhibits a temporal coherence comparable with that of HEVC, while offering more detailed textures. As a result, we outperform HEVC on perceptual quality at lower bit-rates. The contributions of this paper are summarized as:

- We propose a novel perceptual video compression approach with recurrent conditional GAN, which learns to compress video and generate photo-realistic and temporally coherent compressed frames.

- We propose adversarial loss functions for perceptual video compression to balance bit-rate, distortion and perceptual quality.
- The experiments (including user study) show the outstanding perceptual performance of our PLVC approach in comparison with the latest learned and traditional video compression approaches.

2 Related work

Learned image compression. In the past years, learned image compression has gained in popularity. For instance, Ballé *et al.* proposed utilizing the variational auto-encoder for image compression and proposed the factorized [Ballé *et al.*, 2017] and hyperprior [Ballé *et al.*, 2018] entropy models. Later, the auto-regressive entropy models [Minnen *et al.*, 2018; Lee *et al.*, 2019; Cheng *et al.*, 2019] were proposed to improve the compression efficiency. Recently, the coarse-to-fine model [Hu *et al.*, 2020a] and the wavelet-like deep auto-encoder [Ma *et al.*, 2020] were designed to further advance the rate-distortion performance. Besides, there are also the methods with RNN-based auto-encoder [Toderici *et al.*, 2017; Johnston *et al.*, 2018] or conditional auto-encoder [Choi *et al.*, 2019] for variable rate compression. Moreover, Agustsson *et al.* [2019] and Menzter *et al.* [2020] proposed applying GANs for perceptual image compression to achieve photo-realistic compressed images at low bit-rate.

Learned video compression. Inspired by the success of learned image compression, the first end-to-end learned video compression method DVC [Lu *et al.*, 2019] was proposed in 2019. Later, M-LVC [Lin *et al.*, 2020] extended the range of reference frames and beats the DVC baseline. Meanwhile, a plenty of learned video compression methods with bi-directional prediction [Djelouah *et al.*, 2019], one-stage flow [Liu *et al.*, 2020], hierarchical layers [Yang *et al.*, 2020a] and scale-space flow [Agustsson *et al.*, 2020] were proposed. Besides, methods like the content adaptive model [Lu *et al.*, 2020], resolution-adaptive flow coding [Hu *et al.*, 2020b], the recurrent framework [Yang *et al.*, 2021] and feature-domain compression [Hu *et al.*, 2021] were employed to further improve compression efficiency. All these methods are optimized for PSNR or MS-SSIM. Veerabadran *et al.* [2020] proposed a GAN-based method for perceptual video compression, but has not outperformed x264 and x265 on LPIPS. Therefore, video compression aimed at perceptual quality still offers room for improvement.

3 Proposed PLVC approach

3.1 Motivation

A GAN was first introduced by Goodfellow *et al.* [2014] for image generation. It learns to generate photo-realistic images by optimizing the adversarial loss

$$\min_G \max_D \mathbb{E}[f(D(\mathbf{x}))] + \mathbb{E}[g(D(G(\mathbf{y})))] \quad (1)$$

where f and g are scalar functions, and G maps the prior \mathbf{y} to $p_{\mathbf{x}}$. We define \mathbf{x} as the groundtruth image and $\hat{\mathbf{x}} = G(\mathbf{y})$ as the generated image. The discriminator D learns to distinguish $\hat{\mathbf{x}}$ from \mathbf{x} . In the adversarial training, it pushes the

distribution of generated samples $p_{\hat{\mathbf{x}}}$ to be similar to $p_{\mathbf{x}}$. As a result, G learns to generate photo-realistic images.

Later, the conditional GAN [Mirza and Osindero, 2014] was proposed to generate images *conditioned* on prior information. Defining the conditions as \mathbf{c} , the loss function can be expressed as

$$\min_G \max_D \mathbb{E}[f(D(\mathbf{x} | \mathbf{c}))] + \mathbb{E}[g(D(\hat{\mathbf{x}} | \mathbf{c}))] \quad (2)$$

with $\hat{\mathbf{x}} = G(\mathbf{y})$. The goal of employing \mathbf{c} in (2) is to push G to generate $\hat{\mathbf{x}} \sim p_{\hat{\mathbf{x}}|\mathbf{c}}$ with the *conditional* distribution tending to be the same as $p_{\mathbf{x}|\mathbf{c}}$. In other words, it learns to fool D to believe that $\hat{\mathbf{x}}$ and \mathbf{x} correspond to a shared prior \mathbf{c} with the same conditional probability. By properly setting the condition prior \mathbf{c} , the conditional GAN is expected to generate frames with desired properties, *e.g.*, rich texture, temporal consistency and coherence, *etc.* This motivated us to propose a conditional GAN for perceptual video compression.

3.2 Framework

Fig. 2 shows the framework of the proposed PLVC approach with recurrent conditional GAN. We define the raw and compressed frames as $\{\mathbf{x}_i\}_{i=1}^T$ and $\{\hat{\mathbf{x}}_i\}_{i=1}^T$, resp. In our PLVC approach, we first estimate the motion between the current frame \mathbf{x}_i and its previous compressed frame $\hat{\mathbf{x}}_{i-1}$ by the pyramid optical flow network [Ranjan and Black, 2017]. The motion is denoted as \mathbf{m}_i , which is to be used in the recurrent generator (G) for compressing \mathbf{x}_i and also to serve as one of the temporal conditions in the recurrent conditional discriminator (D). The architectures of G and D in our PLVC approach are introduced next.

Recurrent generator G . The recurrent generator G plays the role as a compression network. That is, given the reference frame $\hat{\mathbf{x}}_{i-1}$ and the motion \mathbf{m}_i , the target frame \mathbf{x}_i can be compressed by an auto-encoder-based DNN, which compresses \mathbf{x}_i to a latent representation \mathbf{y}_i and outputs the compressed frame $\hat{\mathbf{x}}_i$. In our PLVC approach, we employ the recurrent compression model RLVC [Yang *et al.*, 2021] as the backbone of G , which contains the recurrent auto-encoders to compress the motion and the residual, and the recurrent probability model P for the arithmetic coding of \mathbf{y}_i . The detailed architecture of G is shown in the *Supplementary Material*¹.

Recurrent conditional discriminator D . The architecture of the proposed recurrent conditional discriminator D is shown in Fig. 2. First, we follow [Menzter *et al.*, 2020] to feed \mathbf{y}_i as the spatial condition to D . This way, D learns to distinguish the groundtruth and compressed frames based on the shared spatial feature \mathbf{y}_i , and therefore pushes G to generate $\hat{\mathbf{x}}_i$ with spatial features similar to \mathbf{x}_i .

More importantly, the temporal coherence is essential for visual quality. We insert a ConvLSTM layer in D to recurrently transfer the temporal information along time steps. The hidden state \mathbf{h}_i^D can be seen as a long-term temporal condition fed to D , facilitating D to recurrently discriminate raw and compressed video taking temporal coherence into consideration. Furthermore, it is necessary to consider the temporal fidelity in video compression, *i.e.*, we expect the motion between compressed frames to be consistent with that

¹<https://arxiv.org/abs/2109.03082>

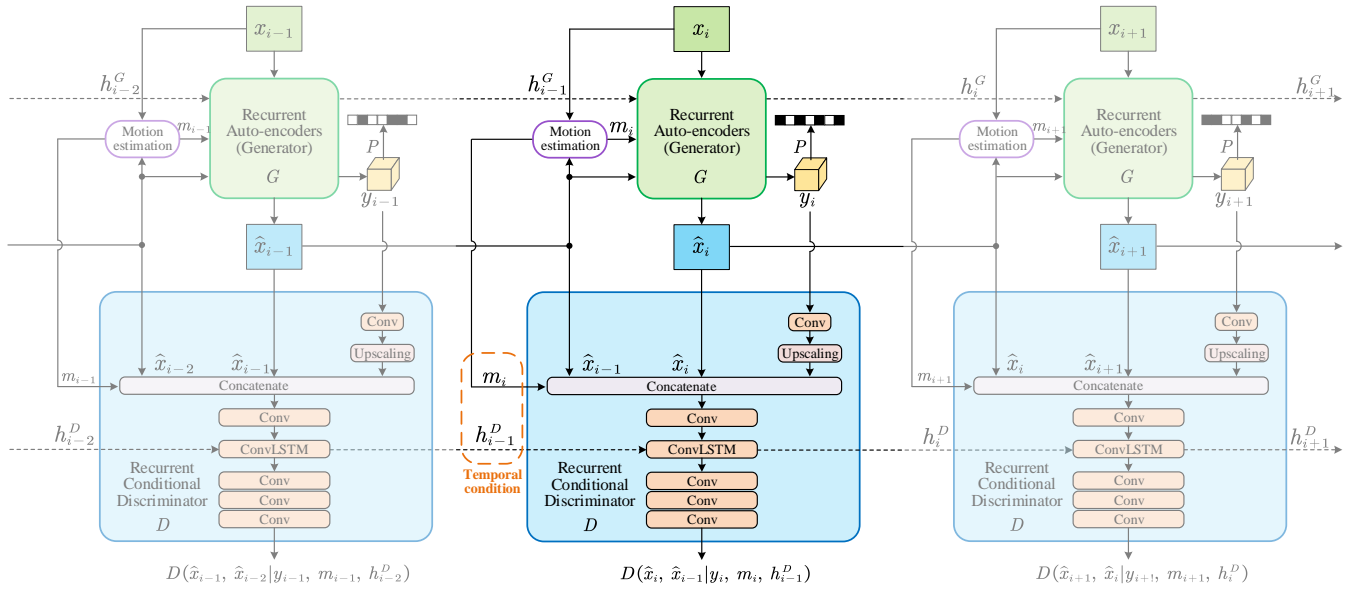


Figure 2: The proposed PLVC approach with recurrent GAN, which includes a recurrent generator G and a recurrent conditional discriminator D . The dash lines indicate the temporal information transferred through the recurrent cells in G and D .

between raw frames. For example, the ball moves along the same path in the videos before and after compression. Hence, we propose D to take as inputs the frame pairs (x_i, x_{i-1}) and $(\hat{x}_i, \hat{x}_{i-1})$ and make the judgement based on the same motion vectors m_i as the short-term temporal condition. Without the m_i -condition, G may learn to generate photo-realistic $(\hat{x}_i, \hat{x}_{i-1})$ but with incorrect motion between the frame pair. This leads to poor temporal fidelity when compared to the groundtruth video. This motivates us to include the temporal condition m_i as an input to the discriminator.

In summary, we propose to condition the discriminator D on spatial features y_i , short-term temporal features m_i and long-term temporal features h_{i-1}^D . Given these conditions, we have $c = [y_i, m_i, h_{i-1}^D]$ in (2) in our PLVC approach. The output of D can be formulated as $D(x_i, x_{i-1} | y_i, m_i, h_{i-1}^D)$ and $D(\hat{x}_i, \hat{x}_{i-1} | y_i, m_i, h_{i-1}^D)$ for the raw and compressed samples, resp. When optimizing the adversarial loss on sequential frames, the compressed video $\{\hat{x}_i\}_{i=1}^T$ tends to have the same spatial-temporal features as the raw video $\{x_i\}_{i=1}^T$. Therefore, we achieve perceptual video compression with spatially photo-realistic as well as temporally coherent frames. Please refer to the *Supplementary Material* for the detailed architecture of D .

It is noteworthy that the effectiveness of D is not restricted to a specific G , but generalizes to various compression networks. Please refer to the analyses and results in Section 4.6.

3.3 Training strategies

Our PLVC model is trained on the Vimeo-90k [Xue *et al.*, 2019] dataset. Each clip has 7 frames, in which the first frame is compressed as an I-frame, using the latest generative image compression approach [Mentzer *et al.*, 2020], and other frames are P-frames. To train the proposed network, we first

Table 1: The hyper-parameters for training PLVC models.

Quality	R_T (bpp)	λ	α_1	α_2	λ'	β
Low	0.025	256	3.0	0.010	100	0.1
Medium	0.050	512	1.0	0.010	100	0.1
High	0.100	1024	0.3	0.001	100	0.1

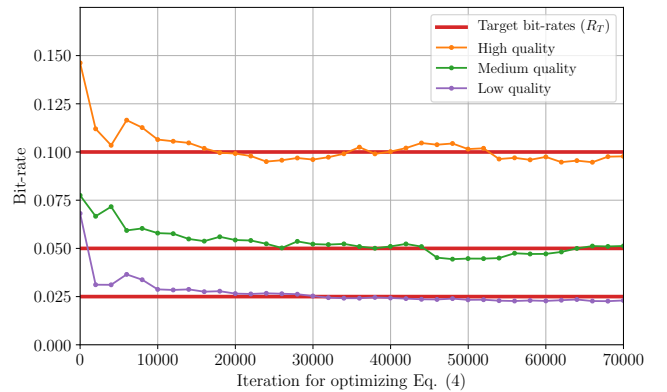


Figure 3: Convergence curves of bit-rates during training.

warm up G on by the rate-distortion loss

$$\mathcal{L}_w = \sum_{i=1}^N R(y_i) + \lambda \cdot d(\hat{x}_i, x_i). \quad (3)$$

In (3), $R(\cdot)$ denotes the bit-rate, and we use the Mean Square Error (MSE) as the distortion term d . Besides, λ is a hyper-parameter to balance the rate and distortion terms.

Then, we train D and G alternately, with the loss function combining the rate-distortion loss and the non-saturating [Lu-

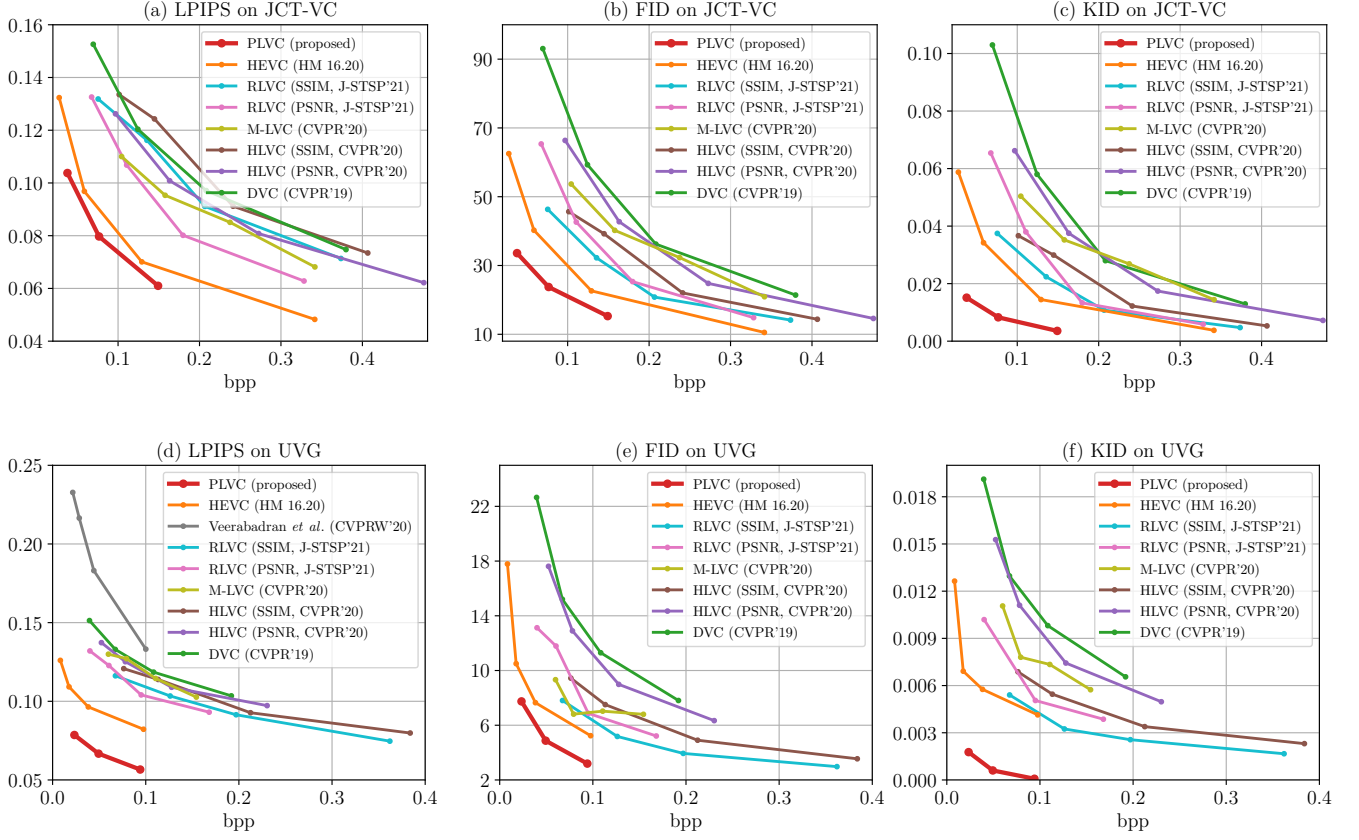


Figure 4: The numerical results on the UVG and JCT-VC datasets in terms of LPIPS, FID and KID.

cic *et al.*, 2018] adversarial loss. Specifically, the loss functions are expressed as follows:

$$\begin{aligned}
 \mathcal{L}_D &= \sum_{i=1}^N \left(-\log \left(1 - D(\hat{\mathbf{x}}_i, \hat{\mathbf{x}}_{i-1} | \mathbf{y}_i, \mathbf{m}_i, \mathbf{h}_{i-1}^D) \right) \right. \\
 &\quad \left. - \log D(\mathbf{x}_i, \mathbf{x}_{i-1} | \mathbf{y}_i, \mathbf{m}_i, \mathbf{h}_{i-1}^D) \right), \\
 \mathcal{L}_G &= \sum_{i=1}^N \left(\alpha \cdot R(\mathbf{y}_i) + \lambda' \cdot d(\hat{\mathbf{x}}, \mathbf{x}) \right. \\
 &\quad \left. - \beta \cdot \log D(\hat{\mathbf{x}}_i, \hat{\mathbf{x}}_{i-1} | \mathbf{y}_i, \mathbf{m}_i, \mathbf{h}_{i-1}^D) \right).
 \end{aligned} \tag{4}$$

In (4), α , λ' and β are hyper-parameters to control the trade-off of bit-rate, distortion and perceptual quality. We set three target bit-rates R_T , and set $\alpha = \alpha_1$ when $R(\mathbf{y}_i) \geq R_T$, and $\alpha = \alpha_2 \ll \alpha_1$ when $R(\mathbf{y}_i) < R_T$ to easily control bit-rates. The hyper-parameters are shown in Table 1. Fig. 3 illustrates the convergence curves of the bit-rates. It can be seen from Fig. 3 that the bit-rates of the PLVC models converge to the target bit-rates during training, showing the effectiveness of our strategy for bit-rate control on the training set.

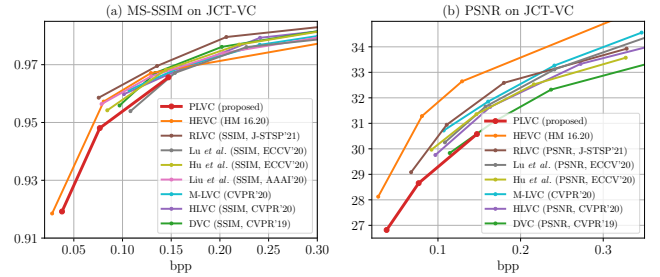


Figure 5: The MS-SSIM and PSNR results on JCT-VC.

4 Experiments

4.1 Settings

We use the JCT-VC [Bossen, 2013] (Classes B, C and D) and the UVG [Mercat *et al.*, 2020] datasets as the test sets. On perceptual metrics, we compare with the Low-Delay P mode of the official HEVC model (HM 16.20) and the latest open-sourced² learned compression approaches DVC [Lu *et al.*, 2019; Yang *et al.*, 2020b]³, HLVC [Yang *et al.*, 2020a], M-LVC [Lin *et al.*, 2020] and RLVC [Yang *et al.*, 2021], and

²We need the codes to reproduce the videos for the user study.

³In this paper, we use OpenDVC [Yang *et al.*, 2020b] to reproduce the results of DVC.

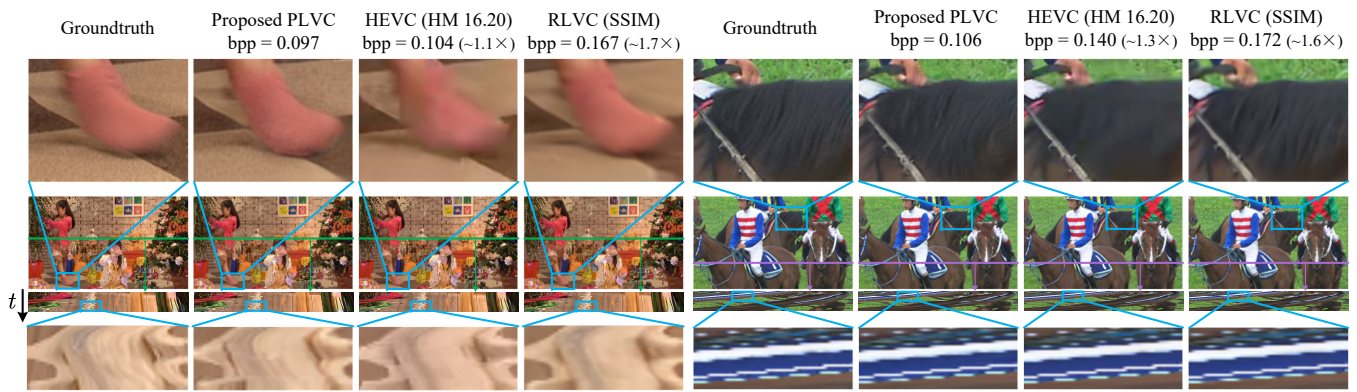


Figure 6: The visual results of the proposed PLVC approach, HM 16.20 and the MS-SSIM-optimized RLVC.

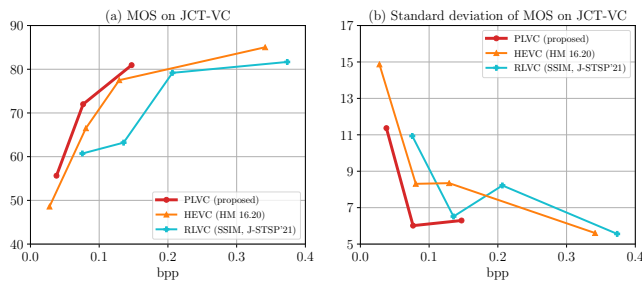


Figure 7: The rate-MOS result and its standard deviation.

the GAN-based method [Veerabadrán *et al.*, 2020]. We also report the MS-SSIM and PSNR results in comparison with several existing approaches. Besides, we conduct MOS experiments as user studies to evaluate perceptual quality. There are 12 non-expert subjects participating in the MOS experiments. They are asked to rate the compressed videos with a score from 0 to 100 according to subjective quality. Higher score indicates better perceptual quality.

4.2 Numerical performance

Perceptual quality. To numerically evaluate the perceptual quality, we calculate the Learned Perceptual Image Patch Similarity (LPIPS) [Zhang *et al.*, 2018], Fréchet Inception Distance (FID) [Heusel *et al.*, 2017] and Kernel Inception Distance (KID) [Bińkowski *et al.*, 2018] on our PLVC and other approaches. In Fig. 4, we observe that the proposed PLVC approach outperforms all compared methods in terms of all three perceptual metrics. Especially, our PLVC approach reaches comparable or even better LPIPS, FID and KID values than other approaches with $2\times$ to $4\times$ the bit-rates of ours. This indicates that PLVC is able to compress video at low bit-rates but with good perceptual quality, showing the efficiency of PLVC for perceptual video compression.

Fidelity. Moreover, Fig. 5 shows that the MS-SSIM of our PLVC approach is comparable with Lu *et al.* [2020]. Our PSNR result also is competitive with DVC. This shows that PLVC is able to maintain the fidelity to an acceptable degree when compressing video. Note that, although MS-SSIM is more correlated with perceptual quality than PSNR, it is still

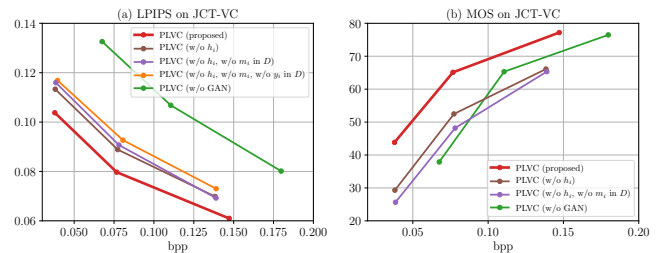


Figure 8: The LPIPS and MOS results of the ablation study. This MOS experiment is independent from Fig. 7 with different subjects, so the MOS values can only be compared within each figure.

an objective metric. In Fig. 5-(a), all learned methods (except M-LVC which does not provide the MS-SSIM-optimized model) are specifically trained with the MS-SSIM loss, resulting in higher MS-SSIM than the proposed PLVC. However, we have shown in Fig. 4 that our PLVC approach performs best in terms of the perceptual metrics. Moreover, the user study in the following section also validates the outstanding perceptual performance of PLVC. This confirms that the perceptual metrics are better than MS-SSIM to evaluate perceptual quality.

4.3 Visual results and user study

Fig. 6 shows the visual results of our PLVC approach in comparison with HM 16.20 and the latest learned approach RLVC [Yang *et al.*, 2021] (MS-SSIM optimized). The top of Fig. 6 illustrates spatial textures, and the bottom shows temporal profiles by vertically stacking the rows along time. It can be seen from Fig. 6 that PLVC yields richer and more photo-realistic textures at lower bit-rates than the methods compared against. Moreover, the temporal profiles indicate that PLVC maintains the temporal coherence comparable to the groundtruth. We provide more visual examples in the *Supplementary Material*⁴.

In the user study, the rate-MOS curves and the standard deviation of MOS for the JCT-VC dataset are shown in Fig. 7. As we can see from Fig. 7-(a), PLVC successfully outperforms the official HEVC test model HM 16.20, especially at

⁴<https://arxiv.org/abs/2109.03082>

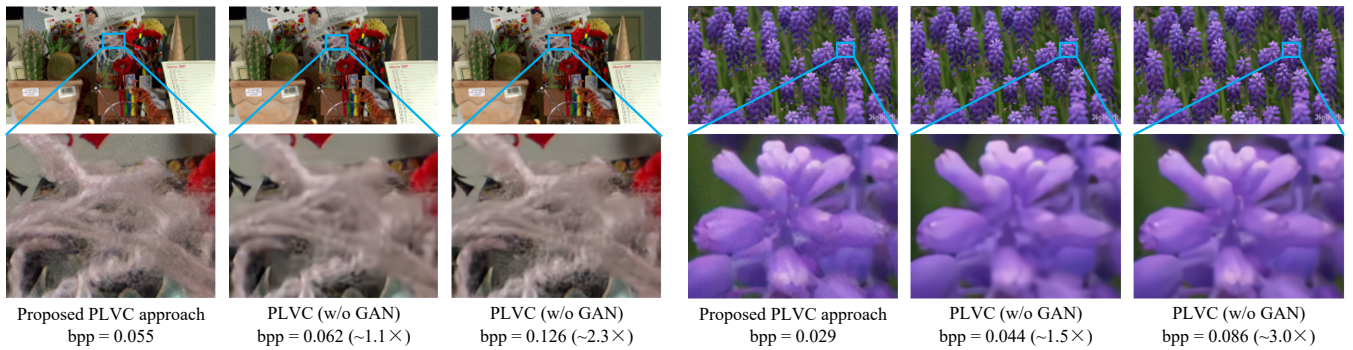


Figure 9: The ablation study on PLVC with and without GAN.

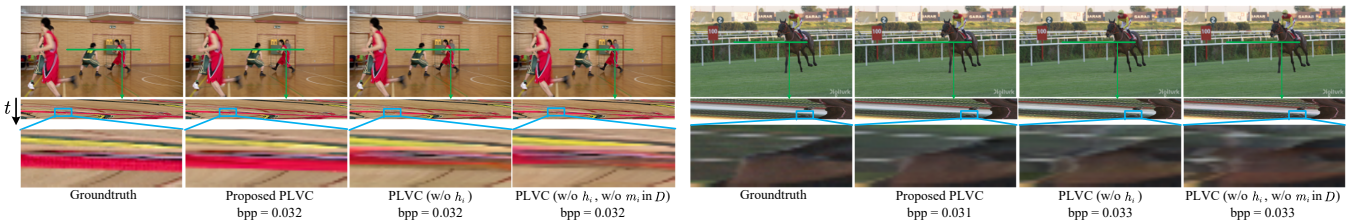


Figure 10: The temporal coherence of the ablation study on the temporal conditions h_i and m_i in D .

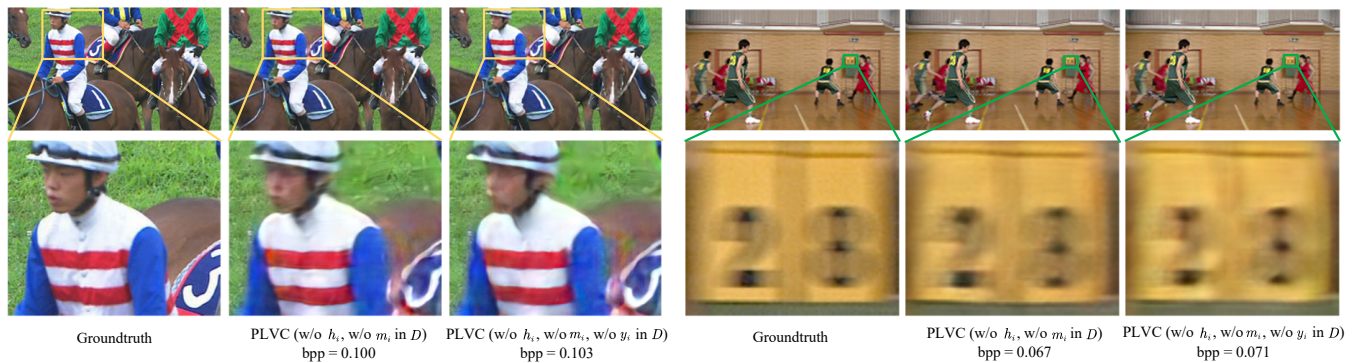


Figure 11: The visual results of the models trained with and without the spatial condition y_i in D .

low bit-rates, and we are significantly better than the MS-SSIM-optimized RLVC. Also, Fig. 7-(b) shows that the standard deviation of MOS values of our PLVC approach is relatively lower than for HM 16.20 and RLVC, indicating that PLVC achieves a more stable perceptual quality. In conclusion, these results confirm that people tend to prefer the perceptual quality of PLVC over that of HM 16.20 and RLVC.

4.4 Ablation studies

In our ablation studies, we analyze the effectiveness of the generative adversarial network, the recurrent structure of the proposed GAN, and the spatial-temporal conditions m_i and y_i . We provide ablation analysis in Fig. 8 in terms of both LPIPS and the MOS of an ablation user study. Note that, the ablation user study is conducted independently of the user study in Fig. 7. The subjects in these two user studies are not the same. Therefore, the MOS values can only be compared within each figure.

Generative adversarial network. We illustrate the results of the distortion-optimized PLVC model, denoted as PLVC (w/o GAN) in Fig. 9, compared with the proposed PLVC approach. The model of PLVC (w/o GAN) is trained only until the convergence of (3) without the adversarial loss in (4). It can be seen from Fig. 9 that the proposed PLVC approach achieves richer textures and more photo-realistic frames than PLVC (w/o GAN), even when PLVC (w/o GAN) consumes $2\times$ to $3\times$ bit-rates. This is also verified by the LPIPS and MOS performance in Fig. 8.

Recurrent GAN. We first remove the recurrency in the proposed GAN (PLVC (w/o h_i)), *i.e.* without the hidden information transferred through the recurrent cells. As we can see from Fig. 10, the temporal profile of PLVC (w/o h_i) (third column) is obviously distorted in comparison with the proposed PLVC approach and the groundtruth. As shown in Fig. 8, the LPIPS and MOS performances of PLVC (w/o h_i) also degrade in comparison with the proposed PLVC model.

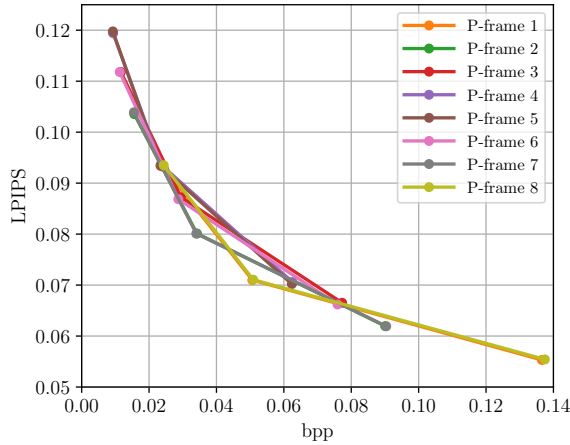


Figure 12: The average performance on each P-frame in GOPs.

Temporal condition m_i in D . We further remove the temporal condition m_i from D and denote it as PLVC (w/o h_i , w/o m_i in D). As such, D becomes a normal discriminator *independent* along time steps. It can be seen from the right column of each example in Fig. 10 that the temporal coherence becomes even worse when further removing the m_i condition in D . Similar result can also be observed from the quantitative and MOS results in Fig. 8. These results indicate that the long-term and short-term temporal conditions h_i and m_i are effective in enabling D to judge raw and compressed videos according to temporal coherence, in addition to spatial texture. This way, it is able to force G to generate temporally coherent and visually pleasing videos, thus resulting in good perceptual quality.

Note that in Fig. 8 the MOS values of PLVC (w/o h_i) and PLVC (w/o h_i , w/o m_i in D) are even lower than those of PLVC (w/o GAN) at some bit-rates. This is probably because the incoherent frames generated by PLVC without temporal conditions h_i and/or m_i severely degrade the perceptual quality, making it even worse than the distortion-optimized model.

Spatial condition y_i in D . Fig. 8 shows that when further removing y_i from the conditions of D (denoted as PLVC (w/o h_i , w/o m_i , w/o y_i in D)), the performance in terms of LPIPS degrades further. We also show visual results in Fig. 11. It can be seen that, compared to PLVC (w/o h_i , w/o m_i in D), the compressed frames generated by PLVC (w/o h_i , w/o m_i , w/o y_i in D) exhibit more artifacts and color shifts (the right example in Fig. 11). This suggests that the spatial condition in D is effective for pushing the generator G to generate compressed frames with spatial features closer to the groundtruth. It boosts the fidelity of the compressed video and improves the visual quality.

4.5 GOP structure and error propagation

In PLVC, we follow RLVC to use the bi-IPPP [Yang *et al.*, 2021] structure with the GOP size of nine frames (one I-frame and eight P-frames). Fig. 12 shows the average LPIPS-bpp curve for each of the eight P-frames in GOPs. The performance is averaged among all GOPs in the JCT-VC dataset.

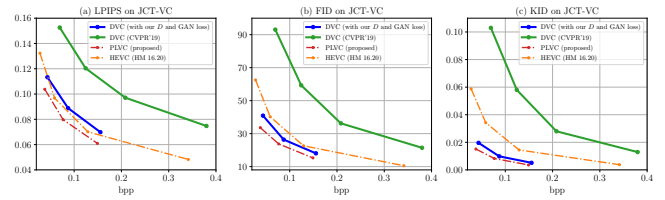


Figure 13: Applying the proposed D and GAN loss to DVC.

There is no obvious error propagation in the P-frames for PLVC. The possible reasons may be two-fold. On the one hand, the bi-IPPP structure shortens the distance between I-frames and P-frames, resulting in less error propagation. On the other hand, thanks to the recurrent structure of PLVC, the hidden states contain richer temporal priors when the distance to I-frames increases. This is beneficial for compression performance, and, hence, can combat error propagation.

4.6 Generalizability of the proposed D

Recall that in PLVC, we utilize RLVC [Yang *et al.*, 2021] as the backbone of G . However, the proposed recurrent conditional discriminator D generalizes to various compression networks. For instance, Fig. 13 shows the results of the DVC trained with the proposed D and GAN loss (blue curve) compared with the original DVC (green curve). It can be seen that the proposed D and GAN loss significantly improve the perceptual performance from the original DVC and make it outperform HM 16.20 on FID and KID. This shows that the proposed approach is not restricted to a specific compression network, but can be generalized to different backbones. It is worth mentioning that DVC trained with the proposed D performs worse than PLVC, because DVC does not contain recurrent cells, while PLVC has a recurrent G which works with the recurrent conditional D , and they together make up the proposed recurrent GAN. As a result, PLVC outperforms the previous traditional and learned video compression approaches on LPIPS, FID, KID and MOS.

5 Conclusion

This paper proposes a GAN-based perceptual video compression approach. Its recurrent generator learns to compress video with coherent and visually pleasing frames to fool the recurrent discriminator, which learns to assess the raw vs. compressed videos conditioned on spatial-temporal features. An adversarial loss function is designed to train the proposed model towards the trade-off among bit-rate, distortion and perceptual quality. The numerical results and user studies both validate the good perceptual performance of the proposed method, in comparison with the traditional video coding standard HM 16.20 and the learned video compression methods.

Acknowledgments

This work was supported by the ETH Zürich General Fund and by Humboldt Foundation.

References

- [Agustsson *et al.*, 2019] Eirikur Agustsson, Michael Tschannen, Fabian Mentzer, Radu Timofte, and Luc Van Gool. Generative adversarial networks for extreme learned image compression. In *ICCV*, 2019.
- [Agustsson *et al.*, 2020] Eirikur Agustsson, David Minnen, Nick Johnston, et al. Scale-space flow for end-to-end optimized video compression. In *CVPR*, 2020.
- [Ballé *et al.*, 2017] Johannes Ballé, Valero Laparra, and Eero P Simoncelli. End-to-end optimized image compression. In *ICLR*, 2017.
- [Ballé *et al.*, 2018] Johannes Ballé, David Minnen, Saurabh Singh, Sung Jin Hwang, and Nick Johnston. Variational image compression with a scale hyperprior. In *ICLR*, 2018.
- [Bińkowski *et al.*, 2018] Mikołaj Bińkowski, Dougal J Sutherland, Michael Arbel, and Arthur Gretton. Demystifying MMD GANs. In *ICLR*, 2018.
- [Bossen, 2013] Frank Bossen. Common test conditions and software reference configurations. *JCTVC-L1100*, 2013.
- [Cheng *et al.*, 2019] Zhengxue Cheng, Heming Sun, Masaru Takeuchi, and Jiro Katto. Learning image and video compression through spatial-temporal energy compaction. In *CVPR*, 2019.
- [Choi *et al.*, 2019] Yoojin Choi, Mostafa El-Khamy, and Jungwon Lee. Variable rate deep image compression with a conditional autoencoder. In *ICCV*, 2019.
- [Djelouah *et al.*, 2019] Abdelaziz Djelouah, Joaquim Campos, et al. Neural inter-frame compression for video coding. In *ICCV*, 2019.
- [Goodfellow *et al.*, 2014] Ian J Goodfellow, Jean Pouget-Abadie, Mehdi Mirza, et al. Generative adversarial nets. In *NeurIPS*, 2014.
- [Heusel *et al.*, 2017] Martin Heusel, Hubert Ramsauer, et al. GANs trained by a two time-scale update rule converge to a local nash equilibrium. In *NeurIPS*, 2017.
- [Hu *et al.*, 2020a] Yueyu Hu, Wenhan Yang, and Jiaying Liu. Coarse-to-fine hyper-prior modeling for learned image compression. In *AAAI*, 2020.
- [Hu *et al.*, 2020b] Zhihao Hu, Zhenghao Chen, Dong Xu, et al. Improving deep video compression by resolution-adaptive flow coding. In *ECCV*, 2020.
- [Hu *et al.*, 2021] Zhihao Hu, Guo Lu, and Dong Xu. FVC: A new framework towards deep video compression in feature space. In *CVPR*, 2021.
- [Johnston *et al.*, 2018] Nick Johnston, Damien Vincent, David Minnen, et al. Improved lossy image compression with priming and spatially adaptive bit rates for recurrent networks. In *CVPR*, 2018.
- [Lee *et al.*, 2019] Jooyoung Lee, Seunghyun Cho, and Seung-Kwon Beack. Context-adaptive entropy model for end-to-end optimized image compression. In *ICLR*, 2019.
- [Lin *et al.*, 2020] Jianping Lin, Dong Liu, Houqiang Li, and Feng Wu. M-LVC: multiple frames prediction for learned video compression. In *CVPR*, 2020.
- [Liu *et al.*, 2020] Haojie Liu, Lichao Huang, Ming Lu, Tong Chen, and Zhan Ma. Learned video compression via joint spatial-temporal correlation exploration. In *AAAI*, 2020.
- [Lu *et al.*, 2019] Guo Lu, Wanli Ouyang, Dong Xu, et al. DVC: An end-to-end deep video compression framework. In *CVPR*, 2019.
- [Lu *et al.*, 2020] Guo Lu, Chunlei Cai, Xiaoyun Zhang, et al. Content adaptive and error propagation aware deep video compression. In *ECCV*, 2020.
- [Lucic *et al.*, 2018] Mario Lucic, Karol Kurach, Marcin Michalski, et al. Are GANs created equal? A large-scale study. In *NeurIPS*, 2018.
- [Ma *et al.*, 2020] Haichuan Ma, Dong Liu, Ning Yan, et al. End-to-end optimized versatile image compression with wavelet-like transform. *IEEE Transactions on Pattern Analysis and Machine Intelligence*, 2020.
- [Mentzer *et al.*, 2020] Fabian Mentzer, George D Toderici, Michael Tschannen, and Eirikur Agustsson. High-fidelity generative image compression. *NeurIPS*, 33, 2020.
- [Mercat *et al.*, 2020] Alexandre Mercat, Marko Viitanen, and Jarno Vanne. UVG dataset: 50/120fps 4K sequences for video codec analysis and development. In *ACM MM-Sys*, 2020.
- [Minnen *et al.*, 2018] David Minnen, Johannes Ballé, and George D Toderici. Joint autoregressive and hierarchical priors for learned image compression. In *NeurIPS*, 2018.
- [Mirza and Osindero, 2014] Mehdi Mirza and Simon Osindero. Conditional generative adversarial nets. *arXiv preprint arXiv:1411.1784*, 2014.
- [Ranjan and Black, 2017] Anurag Ranjan and Michael J Black. Optical flow estimation using a spatial pyramid network. In *CVPR*, 2017.
- [Toderici *et al.*, 2017] George Toderici, Damien Vincent, Nick Johnston, et al. Full resolution image compression with recurrent neural networks. In *CVPR*, 2017.
- [Veerabadrán *et al.*, 2020] Vijay Veerabadrán, Reza Pourreza, et al. Adversarial distortion for learned video compression. In *CVPR Workshops*, 2020.
- [Xue *et al.*, 2019] Tianfan Xue, Baian Chen, Jiajun Wu, et al. Video enhancement with task-oriented flow. *IJCV*, 127(8):1106–1125, 2019.
- [Yang *et al.*, 2020a] Ren Yang, Fabian Mentzer, et al. Learning for video compression with hierarchical quality and recurrent enhancement. In *CVPR*, 2020.
- [Yang *et al.*, 2020b] Ren Yang, Luc Van Gool, and Radu Timofte. OpenDVC: An open source implementation of the dvc video compression method. *arXiv preprint arXiv:2006.15862*, 2020.
- [Yang *et al.*, 2021] Ren Yang, Fabian Mentzer, et al. Learning for video compression with recurrent auto-encoder and recurrent probability model. *IEEE J-STSP*, 2021.
- [Zhang *et al.*, 2018] Richard Zhang, Phillip Isola, Alexei A Efros, et al. The unreasonable effectiveness of deep features as a perceptual metric. In *CVPR*, 2018.

Perceptual Learned Video Compression with Recurrent Conditional GAN

– Supplementary Material –

Ren Yang¹, Radu Timofte^{1,2}, Luc Van Gool^{1,3}

¹ETH Zürich, Switzerland,

²Julius Maximilian University of Würzburg, Germany ³KU Leuven, Belgium

6 Detailed architectures

Fig. 14 shows the detailed architecture of the recurrent generator G . In Fig. 14, the convolutional layers are denoted as “Conv, filter size, filter number”. GDN [Ballé *et al.*, 2017] and ReLU are the activation functions. Note that the layers with ReLU before Conv indicates the pre-activation convolutional layers. $\downarrow 2$ and $\uparrow 2$ are $\times 2$ downscaling and upscaling, respectively. In the quantization layer, we use the differentiable quantization method proposed in [Ballé *et al.*, 2017] when training the models, and use the rounding quantization for test. The Convolutional LSTM (ConvLSTM) layers in the auto-encoders make the proposed G have the recurrent structure.

The detailed architecture of the proposed recurrent conditional discriminator D is illustrated in Fig. 15. The denotations are the same as Fig. 14. In D , we utilize the spectral normalization, which has been proved to be beneficial for discriminator. In the leaky ReLU, we set the leaky slope as 0.2 for negative inputs. Finally, the sigmoid layer is applied to output the probability in the range of $[0, 1]$.

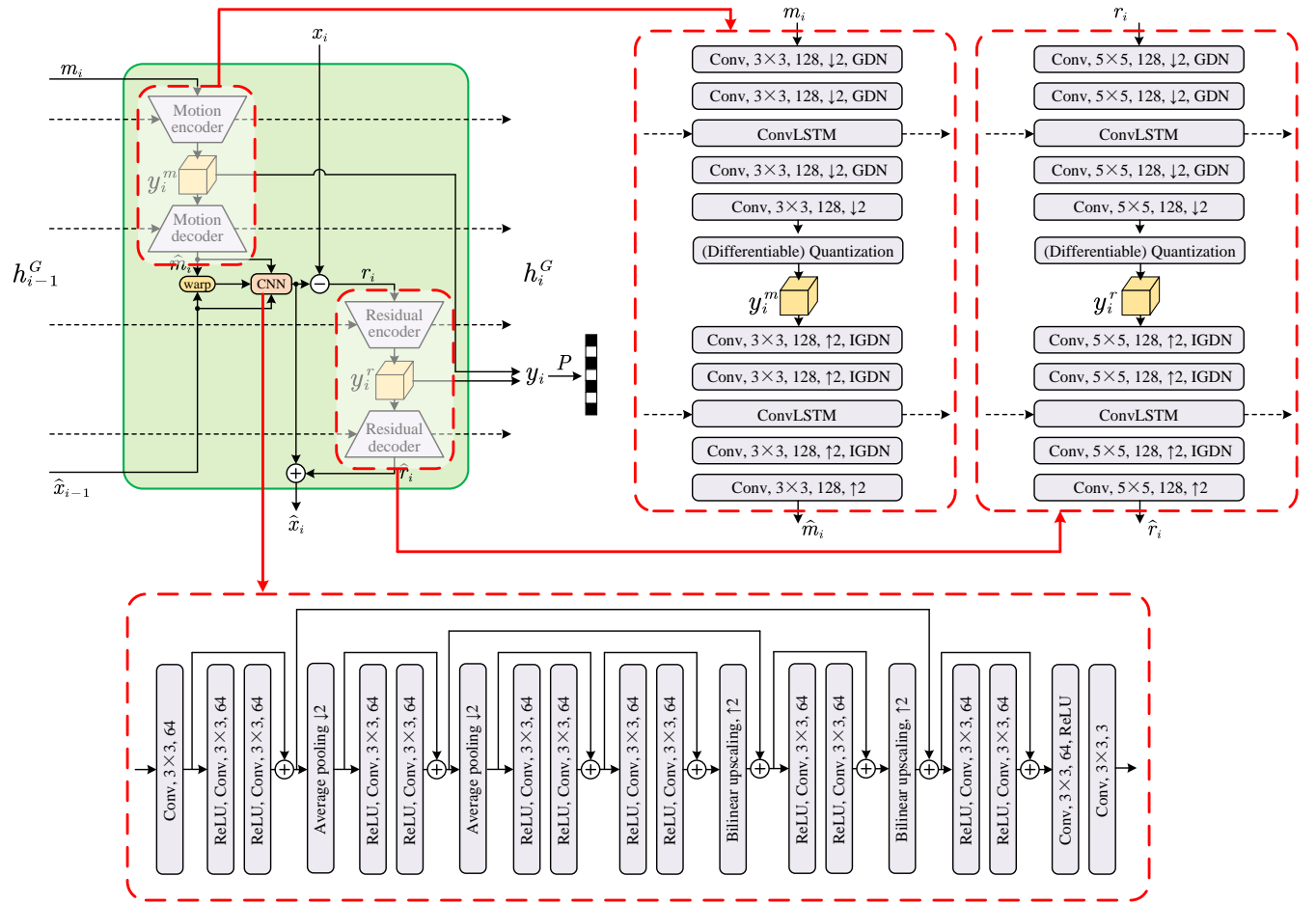


Figure 14: The detailed architecture of the recurrent generator G .

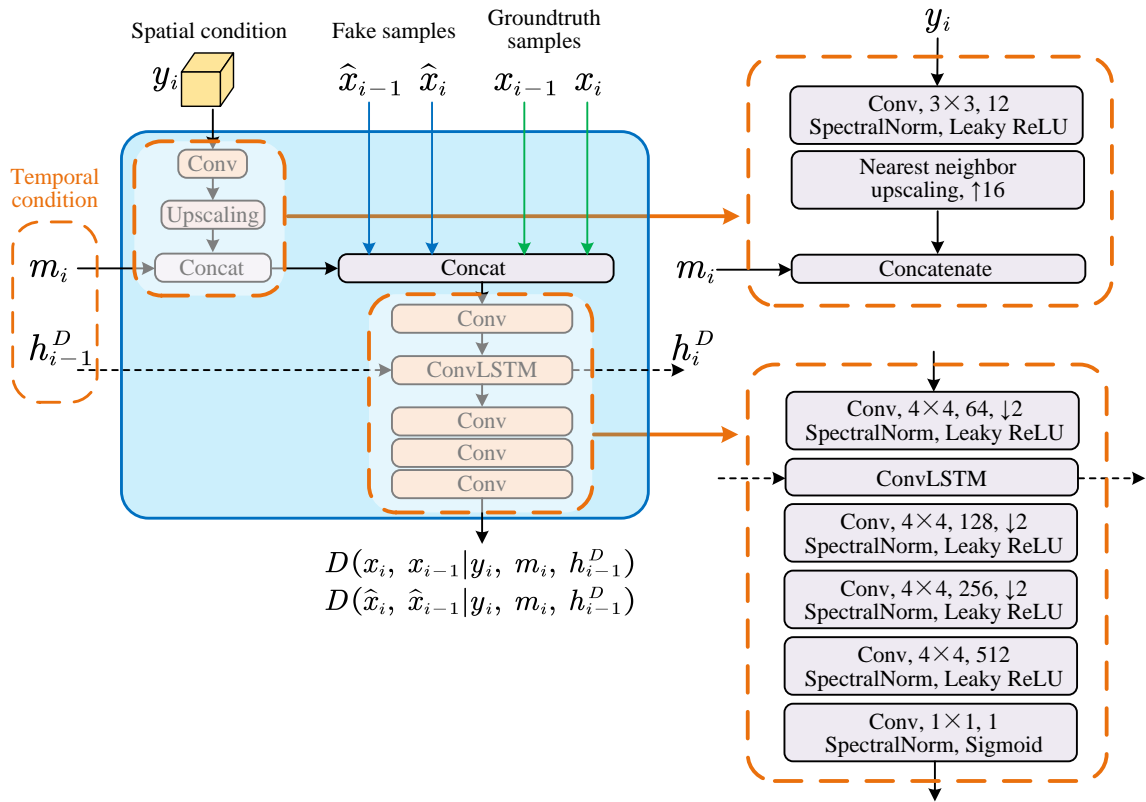


Figure 15: The detailed architecture of the recurrent conditional discriminator D .

7 More visual results

We illustrate more visual results in Fig. 16 (on the *last* page), which shows both spatial textures and temporal profiles of the proposed PLVC approach, HEVC (HM 16.20) and RLVC (MS-SSIM) [Yang *et al.*, 2021], in addition to Fig. 6 in the main text. It can be seen from Fig. 16, the proposed PLVC approach achieves more detailed and sharp textures than other methods, even if when HEVC consumes obviously more bit-rates and RLVC consumes more than $2\times$ bits. Besides, the temporal profiles also show that our PLVC approach has similar temporal coherence to the groundtruth, and the temporal profiles also show that we generate more photo-realistic textures than the compared methods. These results are consistent with the user study in Fig. 7 of the main text, validating the good perceptual performance of the proposed PLVC approach.

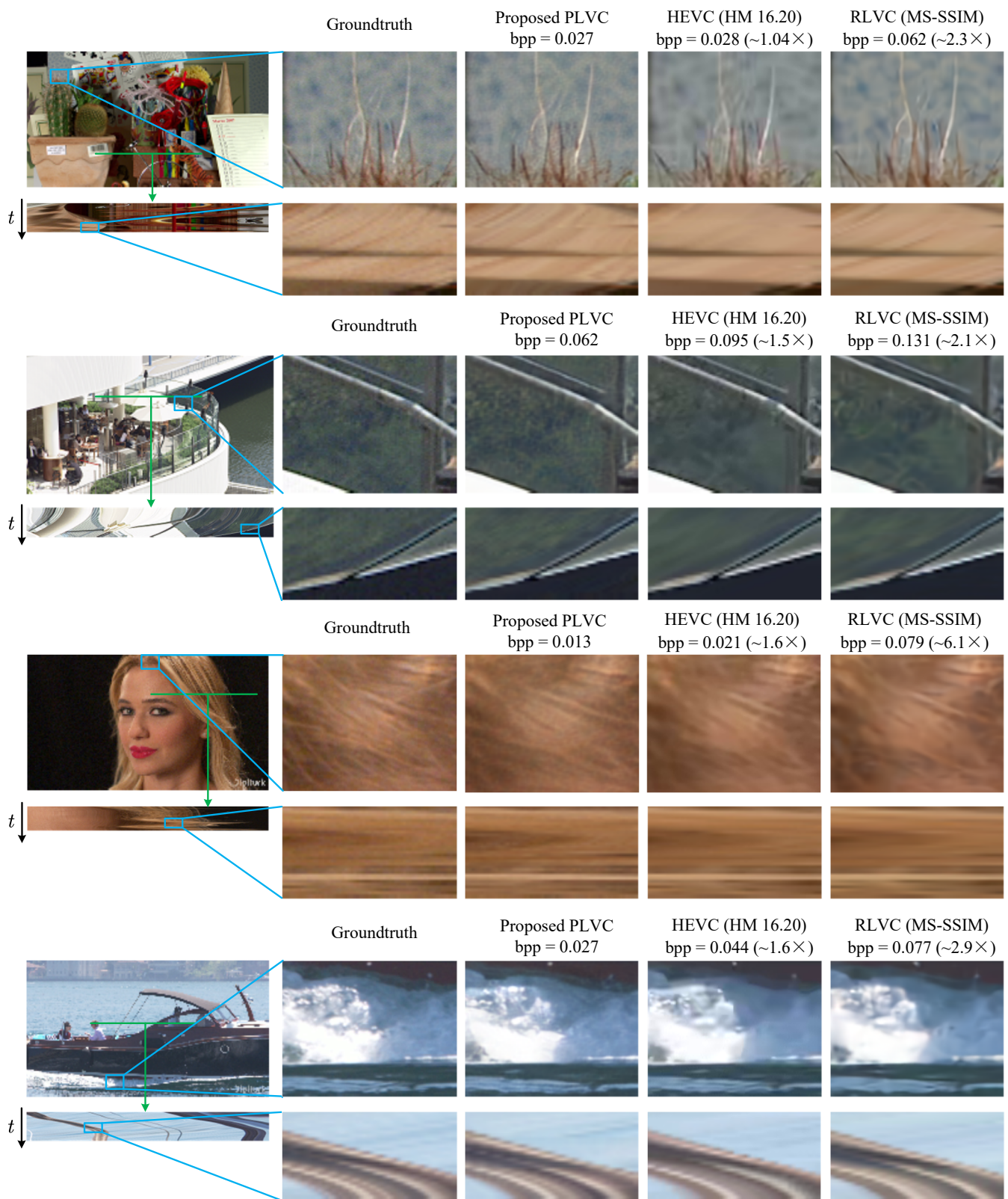


Figure 16: The visual results of the proposed PLVC approach in comparison with HM 16.20 and the MS-SSIM optimized RLVC.